3D Geophysical Inversion for Contact Surfaces

Peter G. Lelièvre and Colin G. Farquharson

Memorial University of Newfoundland, Department of Earth Sciences, St. John's, NL, Canada

Introduction

Geologists' interpretations about the Earth typically involve distinct rock units with contacts between them, e.g. Fig. 1(a). In contrast, standard minimum-structure voxel-based inversions recover smooth models inconsistent with such interpretations, e.g. Fig. 1(b). There are several approaches through which voxel-based geophysical inversion can help recover models with the desired characteristics, e.g. iterative strategies, regularization design, level set methods and clustering strategies [1]. However, the underlying parameterization of the Earth is still inconsistent with geologists' interpretations. **We are researching a fundamentally different type of inversion that parameterizes the Earth in terms of the contact surfaces between rock units.**

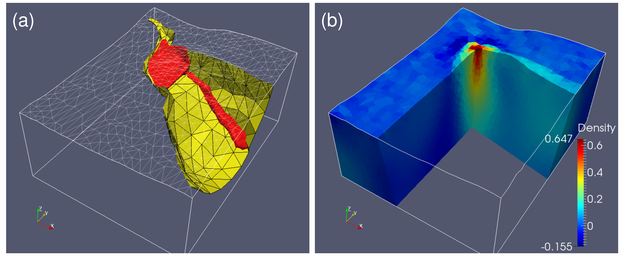

Figure 1 : (a) A geological model from the Voisey's Bay Eastern Deeps deposit, comprising wireframe surfaces of tessellated triangles. Three surfaces are visible: the topography surface is shown as a transparent white wireframe, a sulphide body is shown as a red surface, and a contact between gneiss and troctolite is shown as a yellow surface with black edges highlighting the facets. (b) A typical smooth distribution recovered from minimum-structure voxel-based inversion.

Methods

3D geological Earth models typically comprise wireframe surfaces of tessellated triangles or other polygonal planar facets, e.g. Fig. 1(a). This wireframe representation allows for flexible and efficient generation of complicated geological structures. **In our geophysical inversions, we parameterize the wireframe contact surfaces as the coordinates of the nodes (facet vertices). We solve for the locations of the nodes through a Particle Swarm Optimization strategy [2, 3] and follow this with a more rigorous Metropolis Hastings stochastic sampling to provide statistical information.** These global optimization methods introduce high computational costs; to provide computationally feasible inversion methods, **we reduce the dimensionality of the problem by parameterizing the nodes in a coarse representation of the geological wireframe model and we use surface subdivision [4, 5] to refine further.** This also provides a simple and effective way to regularize the inverse problem.

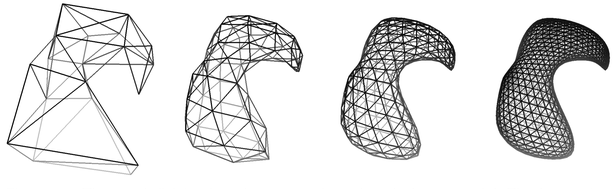

Figure 2 : Three subdivision iterations on a triangular wireframe model. The facet edges are coloured lighter away from the viewer.

Synthetic ellipsoid example

In this and the following section, we invert synthetic gravity gradiometry data collected above two bodies. The data is contaminated with a realistic level of noise prior to inversion. **Our first example, Figs. 3 & 4, involves a dipping isolated body of ellipsoid-like shape.** The control surface is prism-like, defined by 8 nodes. The control surface was subdivided twice to obtain the candidate models. This example is similar to the salt-dome illustrative example presented by [6], in which a relatively simple shape is represented by a wireframe surface and moved using a few shape parameters, e.g. that describe the stem radius, height and thickness of the cap. Our inversion methods provide more flexibility in the ways in which the shape can move and contort. **The recovered model fits well to the true model, with consistent location, orientation and aspect ratios.** The recovery of the deeper end of the body is slightly worse than for the shallower end. This is expected due to the lowered sensitivity of the gradiometry data with increasing depth. The stochastic sampling provides a consistent story, with lower standard deviations closer to the data.

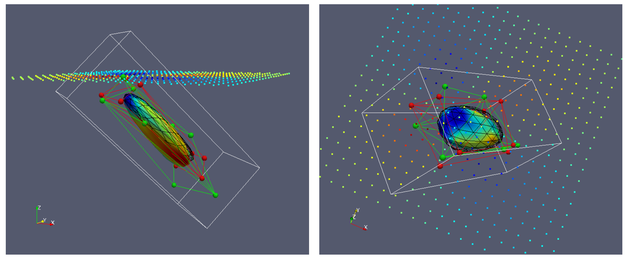

Figure 3 : Inversion results for our synthetic ellipsoid example. The true model is shown as a black wireframe. The control surfaces for the true and recovered models are red and green respectively. The green control nodes were allowed to move within a large volume, shown here in white. The recovered model is coloured by the standard deviations associated with the facet locations (blue low, red high). The data locations are plotted as coloured dots (coloured by the XY component). The view at left is from the side and the view at right from overhead.

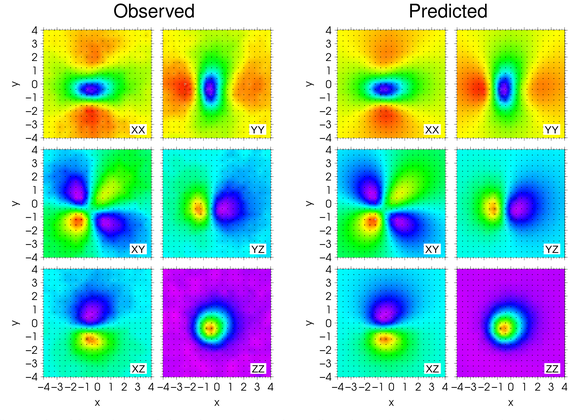

Figure 4 : Map views of the observed and predicted gravity gradiometry data for our synthetic ellipsoid example. Colour scales are identical for each observed and predicted component pair. Black dots indicate data locations.

Synthetic sheet example

Our second example, Figs. 5 & 6, involves an undulating dipping sheet, roughly S-shaped in cross-section, representing part of a 3D geological model. The control surface for the true model is defined by 16 nodes. The control surface for the inversion contains 21 nodes, 9 of which we allowed to move, the remaining 12 define the outline of the sheet and remained stationary in the inversion. Both control surfaces were subdivided twice to obtain the true and candidate models. This example has similar characteristics to the basin geology inversion example presented by [6], in which a roughly horizontal contact between alluvial overburden and bedrock was represented by a wireframe surface. In their example, the nodes in the wireframe surface were allowed to move vertically. Again, in our methods we provide more flexibility in the ways in which the wireframe model can move and contort, and our subdivision strategy ensures that surfaces are recovered with smooth curvatures. **The recovered model follows the true surface well, a promising result for this complicated scenario.**

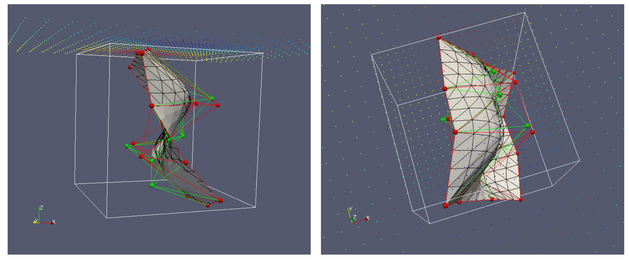

Figure 5 : Inversion results for our synthetic sheet example. The true model is shown as a black wireframe. The control surfaces for the true and recovered models are red and green respectively. The green control nodes were allowed to move within a large volume, shown here in white. The recovered model is coloured grey here to simplify the images. The data locations are plotted as coloured dots (coloured by the XY component). The view at left is from the side and the view at right from overhead.

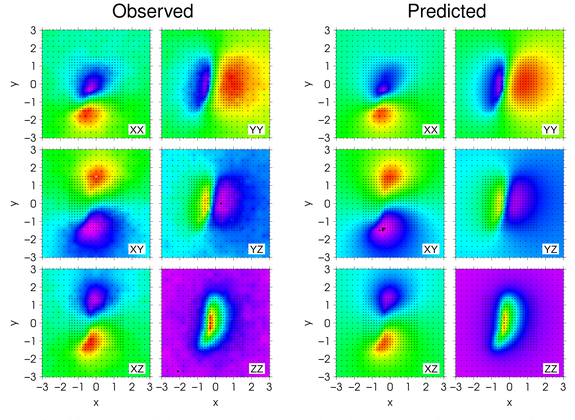

Figure 6 : Map views of the observed and predicted gravity gradiometry data for our synthetic sheet example. Colour scales are identical for each observed and predicted component pair. Black dots indicate data locations.

Real data example

In this example, Fig. 7, we invert gravity data collected above an IOCG deposit in South Australia. IOCG deposits are thought to form as pipe-like or fault-bound hydrothermal breccias. **Our preliminary recovered model is consistent with the understanding of the geology and with voxel inversion results.**

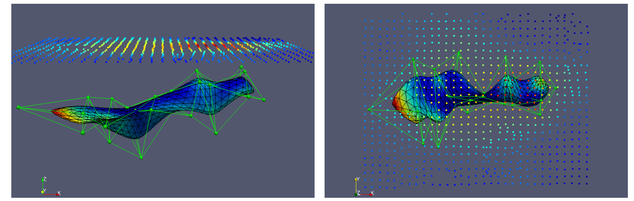

Figure 7 : Inversion results for our real data example. The control surface for the recovered model is green. The recovered model is coloured by the standard deviations associated with the facet locations (blue low, red high). The facets in the recovered surface are outlined in black. The data locations are plotted as coloured dots (coloured by the data values). The view at left is from the south and the view at right from overhead (north up).

Conclusion

We are developing and researching inversion methods that represent the Earth as wireframe surfaces. Such models can better emphasize distinct rock units, and the contacts between them, than typical minimum-structure inversions. Despite the computational challenges involved, methods for parameter reduction and parallelization can be applied to significantly limit computation times. **This work provides computationally feasible approaches for working with subsurface parameterizations that can produce Earth models more compatible with the way geologists typically think of the subsurface.**

Acknowledgements

We thank Jamin Cristall for his help with the real data example. Financial support was provided by the Atlantic Innovation Fund (Atlantic Canada Opportunities Agency), the Natural Sciences and Engineering Research Council of Canada (NSERC), and Vale through the Inco Innovation Centre at Memorial University.

References

[1] P. G. Lelièvre, P. Zheglova, T. Danek, and C. G. Farquharson. Geophysical inversion for contact surfaces. In *SEG Technical Program Expanded Abstracts 2012*, volume 29, pages 1–5, DOI:10.1190/segam2012–0716.1, 2012.

[2] J. Kennedy and R. Eberhart. Particle swarm optimization. In *Proceedings of the IEEE International Conference on Neural Networks*, volume IV, pages 1942–1948, 1995.

[3] R. Poli, J. Kennedy, and T. Blackwell. Particle swarm optimization. *Swarm Intelligence*, 1(1):33–57, 2007.

[4] C. Loop. Smooth subdivision surfaces based on triangles. Master's thesis, University of Utah, 1987.

[5] J. Peters and U. Reif. *Subdivision Surfaces*. Springer Berlin Heidelberg, 2008.

[6] R. M. Richardson and S. C. MacInnes. The inversion of gravity data into three-dimensional polyhedral models. *Journal of Geophysical Research*, 94(B6):7555–7562, June 1989.